C-1.1.4 Study on the Transport and Transformation Model for the Environmental Acidification Substances

Contact person Sato Junji
Atmospheric Environment and Applied Meteorology Research Department
Meteorological Research Institute
1-1Nagamine, Tsukuba, Ibaraki 305-0052, Japan
Tel: +81-298-53-8627 Fax: +81-298-55-7240
E-mail: jsatoh@mri-jma.go.jp

Total Budget for FY1996-FY1998 11,710,000 Yen (FY1998; 3,759,000 Yen)

Abstract In order to examine transboundary transport of sulfur oxides in the east Asian region, two simulation runs were performed during whole year of 1985 over the east Asian region by using the Lagrangian particle model. One simulation was including Japanese domestic emission source, the other was excluding it. Results were compared each other to investigate the impact on deposition of sulfate. In the case to exclude the Japanese domestic emission source, the impact on deposition originating from the Asian continent was seen at several area of Japan.

Keywords: East Asia, Sulfur oxides, Transport, Deposition, Numerical model

1. Introduction

The anthropogenic emission of sulfur oxides has been increased in the east Asian region, it became more than 29 million tones /year at 1987 (Kato et al., 1992). Since the acid deposition becomes serious problem, the east Asian acid deposition monitoring network (EANET) start to operate over the 12 countries of the east Asia at the year of 2000. In present time, it is difficult to estimate the amount of acid deposition due to transboundary transport. One way to circumvent this difficulty is estimation by numerical model.

The long-range transport model of sulfur oxides (MRI-LTM) was developed to evaluate the deposition over the east Asian region (Sato et al., 1995). The MRI-LTM includes the functions to capture deposition and transformation processes of sulfur oxides, but the detailed interaction process between cloud and sulfur oxides is not included.

Since the liquid phase oxidation of sulfur dioxide plays important role in wet deposition process, (Schwaltz, 1988), in order to include the liquid phase oxidation, the MRI-LTM was improved to have the special function expressing wet deposition process in cloud. The main improvements were introduction of the liquid phase oxidation of sulfur dioxide in cloud, and below cloud scavenging process.

2. Outline of the Improved MRI-LTM

The MRI-LTM consists of two main submodels; a meteorological submodel and a dispersion sub- model. The former submodel predicts meteorological variables and the latter includes advection, diffusion, deposition, and chemical transformation processes.

2.1 Meteorological Submodel

Since the meteorological submodel of the MRI-LTM had the spatial resolution of 127km

(FLM: Fine-mesh Limited-area Model), it could not express the cloud process. In order to keep wide model domain as the east Asian region and to gain the higher spatial resolution over focused area, the Spectral Limited-area Model around Japan (JSM) was nested within the FLM by using the spectral coupling method (Sasaki et al., 1995).

i) Outer model

Since the detailed explanation of the FLM was already described by Satomura et al., (1994) and Sato et al., (1995), only outline of the FLM is given here. The outer model consists of 73 grids for longitudinal and 55 grids for latitudinal directions with the interval about 127 km. Topography is put on a polar stereographic projection plane at 60° N. The model atmosphere is divided to 16 layers with the σ coordinate system. The turbulence closure model of level 2 (Mellor and Yamada, 1974) is employed to represent the vertical turbulent diffusion in the planetary boundary layer. The similarity theory is applied to determine vertical fluxes from the ground surface. The governing equations are primitive equations for momentum, mass, specific humidity, and potential temperature using flux forms.

The prognostic variables are wind velocity component for latitudinal and longitudinal directions, u and v, respectively, the potential temperature, θ, the specific humidity, q, and the ground level pressure, π. The vertical velocity σ is obtained diagnostically. Two types of parameterization for the precipitation are made: the large scale condensation parameterization and moist convective adjustment. The former prevents super saturation and the latter keeps the lapse rate between the dry and the moist adiabatic lapse rates. The global objective analysis (GANL) created by the Japan Meteorological Agency is used for the initial and the lateral boundary values for the outer model.

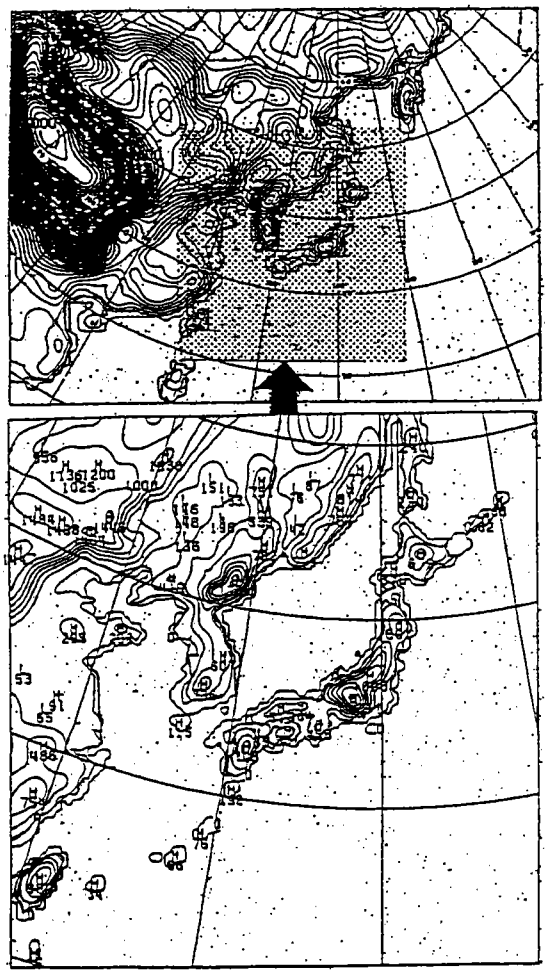

Fig. 1. Domain and topography of the outer model. Inner frame indicates the area of inner model.

ii) Inner model

The JSM is used for inner model whose spectral representation is described by Tatsumi(1986). The inner model is fundamentally similar to the outer model excepting for model domain, spatial resolution, and little physical process. The most dissimilar point is that the radiation process is includes in the inner model. The model has a regular 97× 97 square transform grids with a interval of 40 km on the polar stereographic projection plane at 60° N. The outer model domain including nested inner model domain with topography is shown in Fig. 1. The σ coordinate is also adopted for the 19 layers in vertical. The vertical resolution becomes finer toward

ground surface. The cloud is defined by the relative humidity at each vertical layer by the empirical formula (Ohno et al., 1984). The performance of the nested meteorological submodel is verified by using several observed meteorological data. The observed precipitation data set from the AMeDAS network was used for the validation of precipitation amount and horizontal distribution. Figure 2 shows the time series variations of observed and predicted precipitation averaged over the Kyushu region. The nested meteorological submodel shows good correspondence with observation.

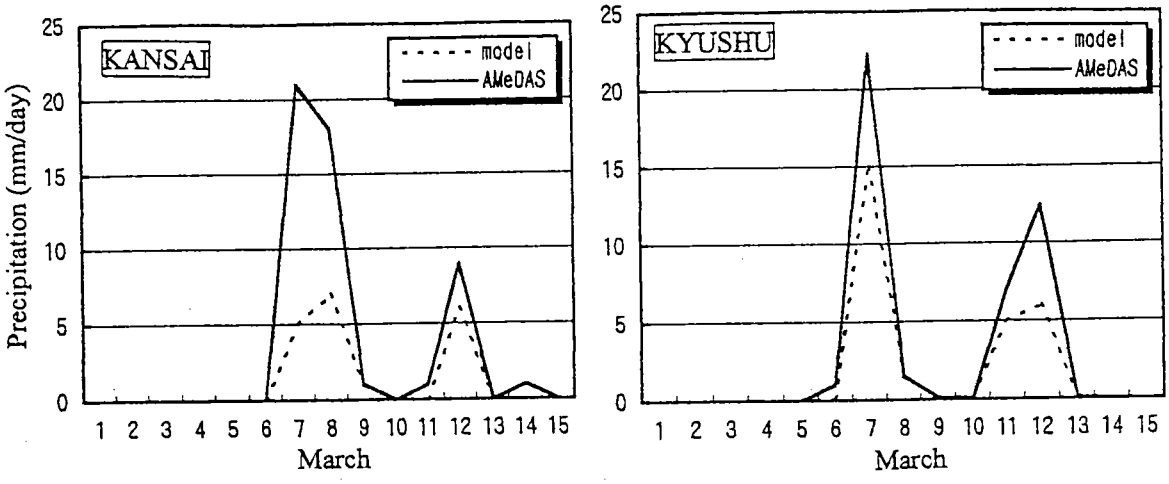

Fig. 2. Time series of predicted and observed precipitation.

2.2. Dispersion Submodel

The dispersion submodel of sulfur oxides is fundamentally based on the mass conservation of sulfur. The motion of a Lagrangian particle with a random walk procedure describes advection and diffusion of these chemical species.

i) Advection and diffusion

The 3-dimensional movement of a particle is calculated using following equations:

$$\frac{dX}{dt} = u, \quad \frac{dY}{dt} = v, \quad \frac{d\sigma}{dt} = \sigma\dot{} + R \tag{1}$$

where, X, Y, and σ are position of a particle on the each coordinate. A random force, R is captured an additional displacement corresponding to the vertical turbulent diffusion. It is defined as:

$$R = \pm\sqrt{2K_z/\delta t} \tag{2}$$

where, δt is the time step in random walk procedure, and the plus or minus sign is chosen randomly for each particle at each time step. The vertical turbulent diffusivity, K_z is derived from meteorological submodel as follows:

$$K_z = l^2\left|\frac{\partial V}{\partial z}\right|F(R_f) \tag{3}$$

l is mixing length represented as

$$l = \frac{kz}{1 + kz/l_0} \tag{4}$$

where, k the Karman constant, and l is proportional to k at the layer close to ground surface and it gradually approach to l_0 with the increase of height, here, l_0 is taken to be equal to 300 m.

ii) Deposition Processes

A particle is assumed to be deposited by a dry process if following two conditions are satisfied; the position of particle is lower than a prescribed height $H_d = 0.99\,\sigma$ in vertical coordinate, and a number given randomly for each particle at each time step is smaller than a value P_d defined as

$$P_d = \frac{V_d \delta t}{H_d} \tag{5}$$

where, V_d is the dry deposition velocity, which varies with meteorological condition, underlying ground surface, and chemical species. Stewart et al., (1983) suggested the dry deposition velocity values over several kinds of ground surface, and Waleck et al., (1986) showed that the dry deposition velocity for SO_2 and SO_4^{2-}, and NO_3 varied with type of ground surface. The simple assumption, therefore, is made. It is that the dry deposition velocities of SO_2 and SO_4^{2-} vary with only two kinds of ground surface conditions, land surface and water surface as seen in Table 1.

Table 1. Dry deposition velocity for SO_2 and SO_4^{2-} as employed in the model.

Species	V_d (cm/sec) land surface	water surface
SO_2	0.51	0.32
SO_4^{2-}	0.21	0.02

Particles are deposited on the surface due to precipitation with a probability of

$$P_w = D_w dt \cdot RR \tag{6}$$

where, D_w is the below cloud scavenging rate, dt the duration to evaluate wet deposition (1 hr), and RR is a precipitation index, which is defined as:

· for particles on grid nodes

$RR=1$, if the predicted precipitation strength exceeds a prescribed threshold value of 0.1mm/hour.

$RR=0$, otherwise.

· for particles between grid nodes

RR is interpolated horizontally using RR around the particle.

Below cloud scavenging rate was suggested by several studies (for instance, Eliassen, 1982; Fisher, 1984), rates are, however, widely scattered between 10^{-5} /sec to 10^{-3} /sec. The constant scavenging rate was assumed in present study. That was $D_w=3\times10^{-5}$/sec for SO_2, and $D_w=1\times10^{-3}$/sec for SO_4^{2-} against stronger precipitation than threshold value. It was assumed that the below cloud scavenging arose below the maximum condensation layer in the inner model. Meanwhile, it was given in whole vertical column at precipitation zone in the outer model, because the outer model had not sufficient spatial resolution to express the maximum condensation layer.

iii) Transformation of SO_2 to SO_4^{2-}

The chemical transformation in present model is that of SO_2 to SO_4^{2-}, because it is difficult to include the detailed chemical reaction in the Lagrangian particle model. The two kinds of transformation rates are considered. One is the gas phase oxidation of SO_2 in the ambient atmosphere, the other is the liquid phase oxidation in cloud. If SO_2 encounter cloud, the liquid phase oxidation is made by prescribed transformation rate. Cox (1974) estimated photo-oxidation of SO_2 in an urban plume with NO_x and hydrocarbons, or thermal oxidation with O_3 and olefin, that was 0.01～0.1/hour. Eliassen and Saltbones (1975) estimates about 0.007/hour. Alkezweeny and Powell (1977) estimated 0.1～0.12/hour from concentration data measured by aircraft. Meagher and Bailey (1983) demonstrated the seasonal variation of SO_2 oxidation from a winter low of 0.0015/hour to a summer high of 0.013/hour. After due consideration of these values, rates of 0.01/hour in the ambient air and 0.07/hour in the cloud (Möller, 1980) were adopted in the present model.

3. Validation of Nesting Effect

In order to valid the nesting effect on transport of particles, a test simulation run was performed for the transport of I^{131} from the accidental release of the Chernobyl nuclear power plant. To examine the behavior of particles around the inner boundary of the nested model, emission source of particles was put at outside of the inner model domain. It was ascertained that particles were smoothly transported through the inner boundary from outer model to inner model domain. The predicted concentration of I^{131} showed good correspondence with observed one.

4. Transport Simulation of Salfur Oxides inn the East Asian Region

The nested model was applied to simulate the transport of sulfur oxides in the east Asian region. In order to evaluate the impact of emission source at the Asian continent on deposition of sulfate around Japan, two simulation runs were performed. One included domestic emission of Japan, the other excluded it.

4.1. Emission Sources

The anthropogenic emission inventory of sulfur oxides for 25 Asian countries east of Afghanistan and Pakistan have been calculated for the years of 1975, 1980, 1985, and 1987 based on the energy consumption (Kato et al., 1992). In addition to the 25 whole countries, province and region-based calculations were made for China and India. The emission inventories based on 1985's in Kato and Akimoto (1992) were redistributed to 66 point sources by Sato et al., (1995) in consideration of industrial activities and population of the major cities. This 66-anthropogenic point source emissions did not include the Japanese domestic emission and Far East of the Russian's. However, the emission source inventories of sulfur over the former Soviet Union territory were given by Ryaboshapko et al., (1998). Then 80-point emission sources including the Japanese domestic emission and Far East of the Russian's were set in present study. But the volcanic and other natural emission sources did not include because of the volcanic emission source is uncertain. Fujita et al., (1993), however, discussed about the emission amount of volcanic sulfur dioxide, and he get conclusion that the amount of sulfur dioxide emitted from the Japanese volcano is comparable to the anthropogenic emission. The emission number and cities are shown in Table 3.

4.2. Simulation and Results

The transport simulations of sulfur oxides were performed all the year around 1985. Figure 3 shows horizontal distribution of SO_4^{2-} deposition expressed as elementary sulfur in meq/m^2/year. (a) indicates dry deposition, (b) wet deposition and (c) total (dry+wet)

Table 3. Emission number, cities and its latitude and longitude established in the model.

Emission No.	Code	Cities	Lat	Lon
1	C1-1	BEIJING	39. 9	116. 4
2	C2-1	TIANJIN	39. 15	117. 22
3	C3-1	SHIJIAZHUANG	38. 02	114. 5
4	C4-1	TAIYUAN	37. 9	112. 55
5	C4-2	DATONG	40. 1	113. 28
6	C5-1	BAOTOU	40. 5	109. 5
7	C5-2	HUHEHOTO	40. 75	111. 7
8	C6-1	DALIAN	38. 85	121. 55
9	C6-2	ANSHAN	41. 1	122. 95
10	C6-3	SHANYANG	41. 75	123. 4
11	C6-4	FUSHONG	41. 8	123. 85
12	C7-1	CHANGCHUN	43. 9	122. 25
13	C7-2	JIRIN	43. 85	126. 5
14	C8-1	HARBIN	45. 75	126. 55
15	C8-2	QIQIHAR	47. 3	123. 95
16	C8-3	DAQING	46. 6	124. 95
17	C8-4	JIAMSI	46. 75	130. 35
18	C9-1	SHANGHAI	31. 2	121. 45
19	C10-1	NANKING	32. 05	118. 75
20	C10-2	MAANSHAN	31. 7	118. 45
21	C10-3	WUXI	31. 6	120. 25
22	C11-1	HANGZHOU	30. 22	120. 04
23	C12-1	HEFUI	31. 85	117. 25
24	C12-2	HUAINAN	32. 61	116. 95
25	C13-1	FUZHOU	26. 06	119. 3
26	C13-2	AMOY	24. 41	118. 12
27	C13-3	SANMING	26. 2	117. 6
28	C14-1	NANCHANG	28. 68	115. 9
29	C14-2	GANZHOU	25. 83	114. 88
30	C15-1	JINAN	36. 62	117
31	C15-2	QUINGDAU	36. 08	120. 25
32	C16-1	ZHENGZHOU	34. 75	113. 7
33	C16-2	LUOYANG	34. 7	112. 4
34	C17-1	WUHAN	30. 56	114. 25
35	C18-1	CHANGSHA	28. 2	113
36	C19-1	GUANGZHOU	23. 2	113. 25
37	C19-2	SWATOWU	23. 7	117. 38
38	C20-1	NANNING	22. 8	108. 28
39	C20-2	LIUZHOU	24. 3	109. 12
40	C21-1	CHENGDU	30. 7	104. 05
41	C21-2	CHONGQING	29. 55	106. 5
42	C21-3	LUZHOU	28. 85	105. 3
43	C22-1	QUIYANG	26. 6	106. 7
44	C23-1	KUNMING	25. 05	102. 7
45	C23-2	GEJIU	23. 35	103. 15
46	C24-1	LHASA	29. 85	91. 15
47	C25-1	XIAN	34. 26	108. 9
48	C25-2	YANAN	36. 59	109. 4
49	C26-1	YUMEN	39. 85	97. 45
50	C26-2	LANZHOU	36	103. 85
51	C27-1	XINING	36. 5	101. 65
52	C28-1	YINCHUAN	38. 48	106. 27
53	C29-1	URUMUQI	43. 85	87. 55
54	SK-1	SEOUL	37. 55	127
55	SK-2	PUSAN	35. 1	129
56	SK-3	TAEGU	35. 85	128. 55
57	SK-4	TAEJON	36. 33	127. 4
58	T-1	TAIPEI	25. 05	121. 48
59	T-2	GAOXING	22. 6	120. 25
60	H-1	HONG KONG	22. 35	114. 2
61	I-1	NONGPO	26. 2	91. 8
62	I-2	KINSHANGANJI	26. 3	90. 5
63	TL	UTTARADIT	17	102
64	NK-1	PYONGYANG	39	125. 5
65	NK-2	HAMHUNG	40	127. 5
66	R-1	VLADIVOSTOK	43	132
67	R-2	CHAVAROVSK	48	135
68	R-3	COMSOMOLSK	50. 5	136. 8
69	R-4	JUZNO SACHALINSK	47. 13	142. 6
70	R-5	PETROPAVLOVSK	50. 29	158. 57
71	J-1	KITAKYUSHU	33. 86	130. 8
72	J-2	NOBEOKA	32. 58	131. 6
73	J-3	TOKUYAMA	34. 07	131. 8
74	J-4	KURASHIKI	34. 57	133. 8
75	J-5	OSAKA	34. 67	135. 52
76	J-6	NAGOYA	35. 17	137
77	J-7	SHIMIZU	35. 03	138. 52
78	J-8	TOKYO	35. 67	139. 72
79	J-9	NIIGATA	37. 9	139. 04
80	J-10	TOMAKOMAI	42. 67	141. 65

deposition.

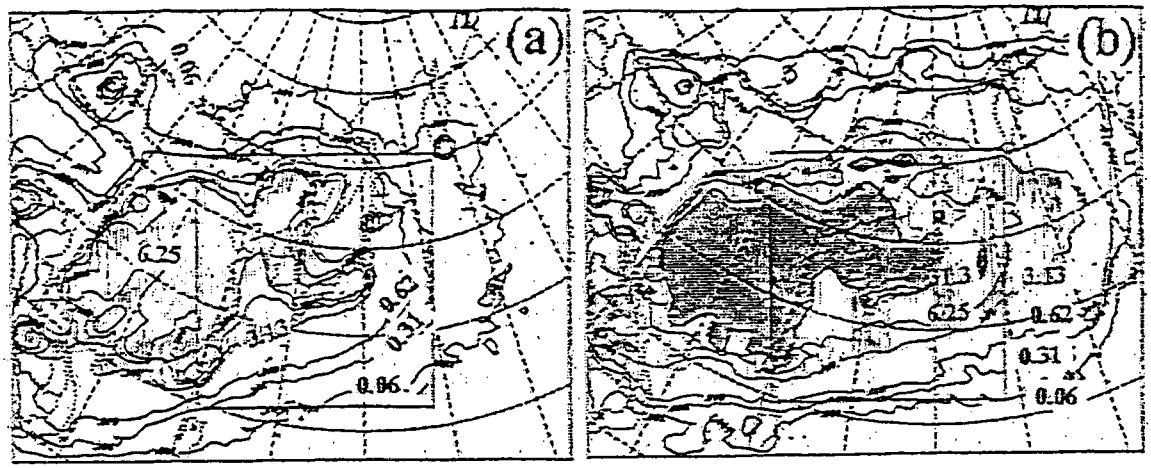

Fig. 3. Horizontal distribution of SO_4^{2-} deposited during the year of 1985 expressed as elemental sulfur in meq/m^2/year. (a) is dry deposition, (b) wet deposition, (c) total deposition, inner frame indicates nested model domain.

As seen in Fig. 3, the model predicted wet deposition to be 30 meq/m^2/year and more over the Japan. The wet deposition of SO_4^{2-} measured at 14 stations in Japan during 1985 shows around 60 meq/m^2/year (see Fig.4).

Since several active volcanoes released SO_2 in Japan, the measured values include the influence by uncertain volcanic emission, which is said to be comparable to anthropogenic emission in Japan (Fujita, et al., 1992). In consideration of the volcanic emission, the model performance shows good correspondence with measured value.

In generally, the atmospheric pressure system is climatically quit different between winter and summer in the east Asian region. Migratory anticyclones frequently pass across the east Asian continent during winter season, and strong northwesterly wind usually prevail around Japan. Therefore, pollutants originated from the Asian continent are transported toward southeast. On the other hand, a large and strong anticyclone persistent over the Pacific Ocean in summer, and weak southerly wind prevail around Japan. This Pacific anticyclone acts to block the transport of pollutants toward southeast. Figure 5 shows two typical horizontal distribution of total SO_4^{2-} deposition during a winter month and a summer month. (a) indicates in a winter month

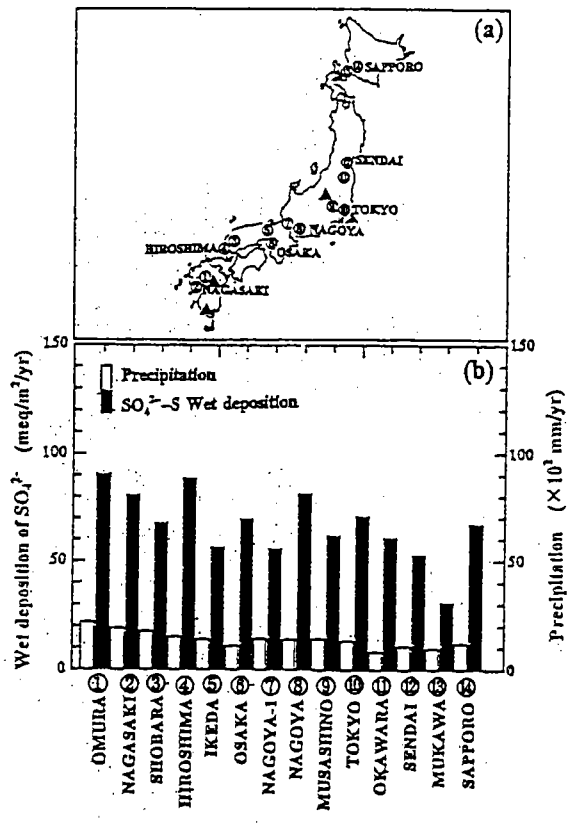

Fig. 4. The location of stations (a) and the measured wet deposition of SO_4^{2-} at 14 stations in Japan (b). The symbol of ▲ shows active volcano.

(January) and (b) in a summer month (August), respectively.

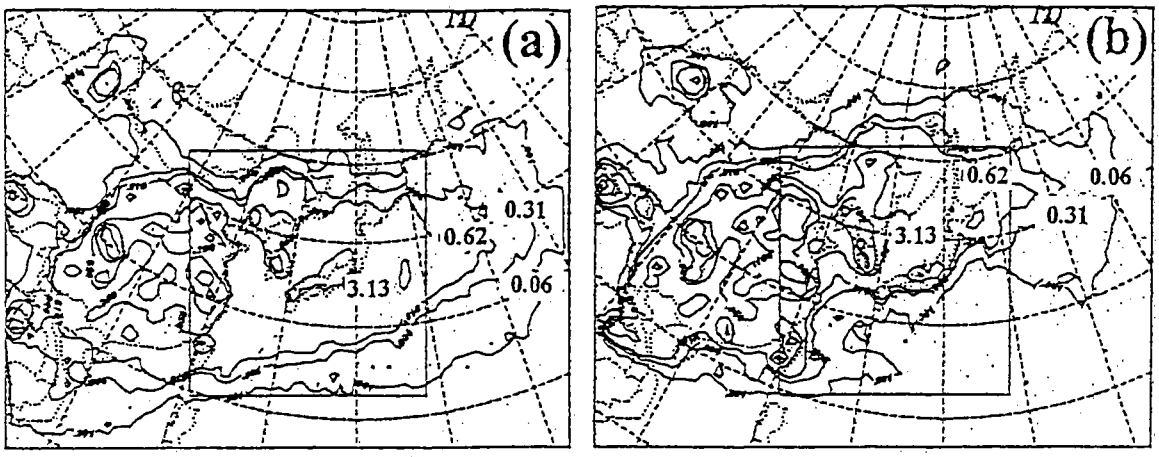

Fig. 5. Two typical horizontal distribution of total SO_4^{2-} deposition. (a) indicates a winter month (January), and (b) in a summer month (August).

As seen in Fig.5, deposition distributes widely eastward in winter, the contribution of Japanese emission sources is, of course, included. In contrast to winter distribution, no deposition arises at eastward of Japan in the summer distribution. And large value of deposition amount arises locally at the Asian continent.

In order to investigate the impact of domestic emission source in Japan on the horizontal distribution of SO_4^{2-} around Japan, two cases of simulation runs were performed. One case included domestic emission sources of sulfur oxides in Japan, the other was excluded it.

The results of two-simulation run were compared by means of SO_4^{2-} deposition in the inner domain. The Japan island is, generally, under the influence of contribution on total deposition originated from the emission sources at Asian continent and Korean peninsula in winter season. But the total deposition caused by the domestic emission sources in Japan is arises widely toward southeast direction, and almost SO_4^{2-} deposit on the Pacific ocean.

Japan is an eminent volcanic country in the world. 67 active volcanoes are dotted within the Japan Islands, and 17 volcanoes are designated as the permanent observation volcanoes by the Japan meteorological Agency. It is

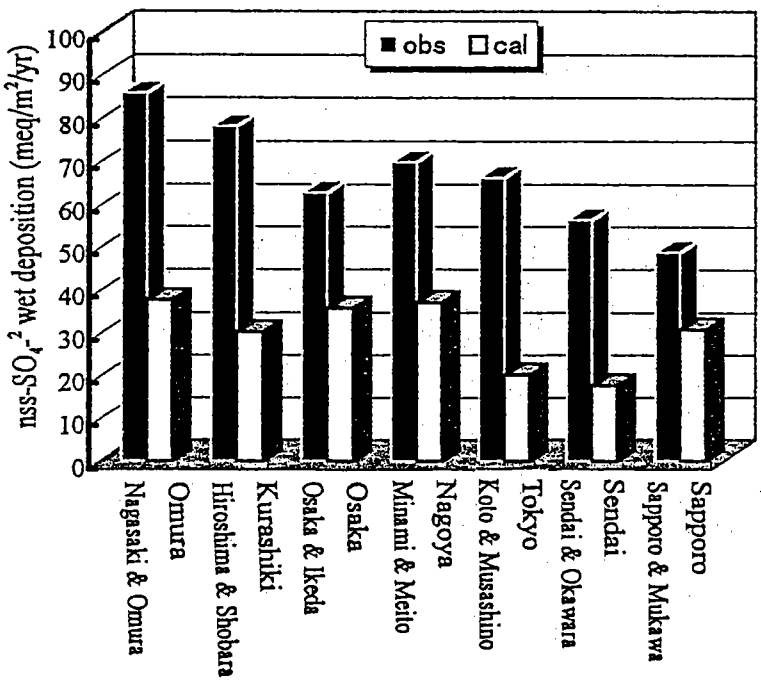

Fig.6. Simulated nss-SO_4^{2-} wet deposition averaged over 80 x 80 km area and measured one averaged two sampling stations.

said that the amount of sulfur dioxide emitted from volcanoes in Japan correspond to the anthropogenic emission of sulfur dioxide (Fujita et al., 1993). On the other hand, the emission of sulfur dioxide originated from volcanoes is excluded in present simulation, because of the volcanic emission depends on activity, so it is very uncertain.

Figure 6 shows simulated wet deposition evaluated at the area of 80 km x 80 km and measured wet deposition averaged at urban and suburb sampling stations. As seen in Fig. 6, simulated wet deposition shows about 50% underestimation. Measurements of wet deposition, however, made by the bulk method, which has the tendency to evaluate less wet deposition. Furthermore, in consideration with sulfur dioxide originated from volcanoes, simulated wet deposition of nss-SO_4^{2-} shows appropriate result. In other words, if additional sulfur dioxide originated from volcano is considered, the long-range transport simulation result will fit to measured wet deposition.

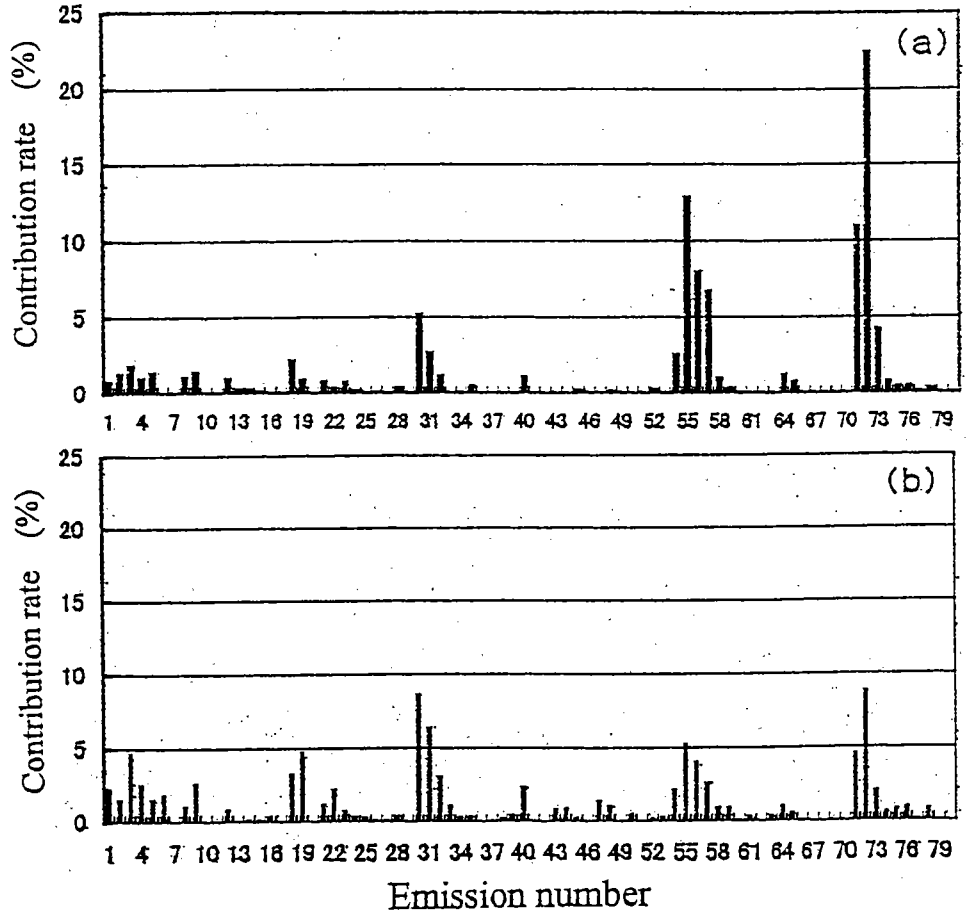

Fig. 7. The simulated ontribution rate from each emission on dry deposition (a) and wet deposition (b) at Omura observation station.

EANET is still going to operate, however, elucidation of a contribution rate from Asian continental emission source depends on a transport model largely. Namely, in order to investigate the source receptor relationship, the Lagrangian particle model suits very well this object. The contribution rate from each emission source is analyzed at the prescribed receptor, here. The contribution rate from each emission source is, firstly, investigated on the deposition at the Omura receptor located on the most west side in Japan, and this station is also situated as receptor in the model. Figure 7 shows contribution rate on the deposition of nss-SO_4^{2-} at the Omura receptor calculated by model. (a) is dry deposition and (b) wet

deposition. Emission source number is the same as shown in Table 3, the largest contribution rate on dry deposition come from the emissions at Nobeoka Kitakyushu and Korea. The influence by emission at Nobeoka on dry deposition occupies about 23 %, but influence on wet deposition is only 9 %.

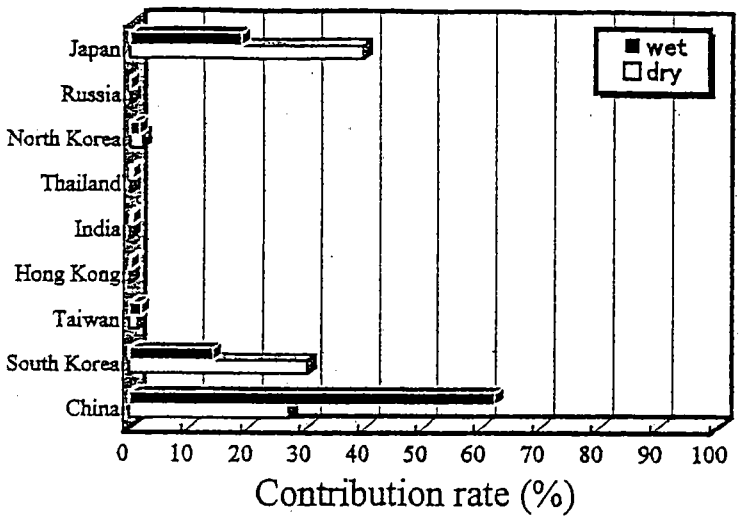

Fig. 8. The contribution rate from whole emission at every country to Omura receptor.

This contribution rate is almost same as Jinan, Shandong province of China. Usually, the contribution rate on wet deposition is strongly influenced by the distant emission source. As seen in Fig. 7, though the contribution from emissions at Kitakyushu and Pusan, Taegu, Taejon of Korea is large, influence by Chines emission is also seen. The contribution rates on dry and wet deposition by every country in east Asian region is shown in Fig. 8. The largest contribution to dry deposition at Omura receptor come from Japanese domestic emission source, the second from Korea, and the third from China. In the case of contribution to wet deposition, the largest contribution is from Chines emission slource, it occupies about 60 %. The second is Japanese domestic emission, about 17 %, the third is Korean emission about 13 %. Contribution from emission source of China is very enormous for wet deposition, difference between contribution rate of emission source at Korea and Japan is small.

5. Concluding Remarks

In order to include liquid phase oxidation process of SO_2 in the cloud, the long range transport was improved. The spectral meteorological model was nested by using spectral boundary coupling method to attain the higher spatial resolution over the focused area. The dispersion submodel also had new function not only liquid phase oxidation but also below cloud scavenging process.

In order to valid the nesting method on a calculation of transport through the inner lateral boundary, test simulation runs were performed. Especially caution was paid on the behavior of particles around inner lateral boundary. Since we got good correspondence with measurements in the validation runs, we performed transport simulation runs of sulfur oxides in the east Asian region for all year, and make clear the transboundary transport process of sulfur oxides originated from the Asian continent. Furthermore, the contribution of the domestic emission sources of Japan becomes also clear.

References

Alkezweeny, A. J. and D. C. Powell, 1977: Estimation of transformation rate of SO_2 to SO_4^{2-} from atmospheric concentration data. *Atmos. Environ.*, **11**, 179-182.

Cox, R. A., 1974: Particle formation from homogeneous reaction of sulfur dioxide and nitrogen dioxide. *Tellus*, **XXVI**, 235-240.

Eliassen, A. and J. Saltbones, 1975: Decay and transformation of SO_2 as estimated from

emission data, trajectory and measured air concentrations. *Atmos. Environ.*, **9,** 425-429.
Fujita, S., Y. Tonooka ans K. Ohta, 1992: Annual contribution of sulfur dioxide emission to the atmosphere in Japan. *J. Japan Soc. Air Pollut.*, **27,** 336-343.
Kato, N. and H. Akimoto, 1992: Anthropogenic emission of SO_2 and NO_x in Asia: Emission inventories. *Atmos. Environ.*, **26A,** 2297-3017.
Meagher, J. F. and E. M. Bailey, 1983: The seasonal variation of the atmospheric SO_2 to SO_4^{2-} conversion rate. *J. Geophys. Res.*, **88,** 1525-1527.
Mellor, G. L. and T. Yamada, 1974: A hierachy of turbulence closure model for planetary boundary layer. *J Atmos. Sci.*, **31,** 1791-1806.
Möller, D., 1980: Kinetic model of ambient SO_4^{2-} oxidation based on published data. *Atmos. Environ.*, **14,** 1067-1076.
Ohno, H. and S. Isa, 1984: A statistical relation between GMS-viewed cloud amount and relative humidity. *Tenki*, **31,** 493-495.
Ryaboshapko, A., L. Gallardo, E. Kjellstöm, S. Gramov, S. Paramonov, O. Afinogenova and H. Rodhe, 1998: Balances of oxidized sulfur and nitrogen over the former Soviet Union territory. *Atmos. Environ.*, **32,** 647-658.
Sasaki, H., H. Kida, T. Koide and M. Chiba, 1995: The performance of long term integration of a Limited Area Model with a spectral boundary coupling method. *J. Met. Soc. Japan,* **73,** 165-181.
Sato, J., T. Satomura, H. Sasaki and Y. Muraji, 1995: The long-range transport model of sulfur oxides and its application to the east Asian region. *Tech. Report of the Met. Res. Inst.* , **No. 34,** 1-101.
Satomura, T., F. Kimura, H. Sasaki, T. Yoshikawa and Y. Muraji, 1994: Numerical simulation of regional scale dispersion of radioactive pollutants from the accident at the Chernobyl nuclear power plant. *Pap. Met. Geophys.*, **45,** 51-63.
Stewart, D. A., R. E. Morris, M. K. Liu and D. Henderson, 1983: evaluation an episodic regional transport model for a multi-day sulfate episode. *Atmos. Environ.*, **17,** 1457-1473.
Tatsumi, Y., 1986: A spectral limited area model with time-dependent lateral boundary condition and its application to a multi-level primitive equation model. *J. Met. Soc. Japan,* **64,** 637-663.
Waleck, C. J. R., R. A. Brost and J. S. chang, 1986: SO_2, sulfate, and HNO_3 deposition velocities computed using regional landuse and meteorological data. *Atmos. Environ.*, **20,** 949-964.